ISSN 1061-933X, Colloid Journal, 2017, Vol. 79, No. 5, pp. 596–604. © Pleiades Publishing, Ltd., 2017.
Original Russian Text © S.I. Grashchenkov, 2017, published in Kolloidnyi Zhurnal, 2017, Vol. 79, No. 5, pp. 553–561.

The Use of the Finite-Element Method for Calculating the Photophoresis Velocity of Large Aerosol Particles

S. I. Grashchenkov
Pskov State University, Pskov, 180000 Russia
e-mail: grasi@mail.ru
Received March 16, 2017

Abstract—The finite-element method has been employed to calculate the photophoresis velocity of solid aerosol particles, the sizes of which are much larger than the mean free path of molecules in a gas. The thermal electromagnetic radiation from the particle surface and the temperature dependences of the density, viscosity, and thermal conductivity of the gaseous medium and particle material have been taken into account. The photophoresis velocity has been numerically calculated for a number of axially symmetric particles moving along their rotation axes. Cylindrical particles, particles having a shape resulting from rhomb rotation around one of its diagonals, and spheroidal particles have been considered.

DOI: 10.1134/S1061933X17050076

INTRODUCTION

Nonuniformly heated aerosol particles are affected by forces that result from the thermal slip of a gas on their surface. When the nonuniform heating of particles is due to the absorption of an electromagnetic radiation by them, the motion induced by these forces is referred to as the photophoresis. This term was proposed by Ehrenhaft [1], who detected the motion of dust particles illuminated by a high-power lamp.

In the case of so-called "large particles," the sizes of which are much larger than the mean free path of gas molecules, the near-particle gas flow may be described within the framework of the continuum model. As a rule, when calculating the distributions of gas temperatures and flow velocities, the Reynolds and Peclet numbers are assumed to be almost equal to zero. For this case, the photophoresis of solid particles was considered in [2, 3]. In these works, the particle heating was believed to be rather weak and the temperature dependences of the molecular-transfer coefficients and gas density were ignored. The velocity and direction of particle motion have been shown to essentially depend on the distribution of internal heat sources [2], which, in turn, depends on the particle size [4]. For metal particles, the absorption of an incident radiation may be believed to occur in a thin surface layer. In this case, the particle velocity is, as a first approximation, independent of the particle size [5], although it is affected by the particle shape [6, 7].

At a rather high intensity of incident radiation, when the temperature dependences of gas-transfer coefficients and density cannot be ignored, the particle velocity becomes size-dependent [8].

Many works, a review of which has been reported in [9], have been devoted to photophoresis. In this study, we shall confine ourselves to a brief review of communications in which the dependences of particle velocity on its shape and degree of heating have been taken into account. In [6], the photophoresis of a particle having the shape of an infinite cylinder and moving in a direction perpendicular to its axis was considered taking into account some corrections for the Knudsen number (the ratio between the mean free path of gas molecules and the characteristic size of a particle). The authors of [10] studied a particle having the shape of a spheroid of revolution and moving under the action of an electromagnetic radiation directed at an arbitrary angle to the spheroid rotation axis. It was supposed that the radiation was absorbed in a thin surface layer of the particle. It has been found that, as the ratio between the lengths of spheroid axes tends to infinity, the velocity of a particle moving under the action of radiation along the major axis also infinitely grows. This result seems questionable, because it entails infinite velocities of the thermal slip on the particle surface. The same problem as in [10] was considered in [7, 11] for flattened spheroids and radiation directed along their rotation axes.

As will be shown below, the photophoresis velocities calculated by the equation derived in [7] coincide with those obtained in this work but differ from the data of [10]. This indicates the invalidation of the results obtained in [10]. The influence of the heating of a particle and, as a consequence, the heating of an ambient gas on the photophoresis velocity of the particle was taken into account in [8, 12–14]. The photo-

phoretic motion of spherical and spheroidal particles was considered in thesis [12] for the case, in which the axial ratio of a flattened spheroid was no higher than two. The calculations were performed for copper particles. For spherical particles, analogous calculations were performed in [8]. In [8, 12], the calculations were carried out using exponential approximations for the temperature dependences of the gas viscosity and the thermal conductivities of the gas and particle material with taking into account the heat radiation from the particle surface. The authors of [13] used the same approximations for the thermal conductivities and viscosities in the case of spherical particles and additionally took into account corrections for the Knudsen number. A similar problem was solved in [14] for a wide range of variations in the Knudsen number with no allowance for the temperature dependence of transfer coefficients but taking into account the heat radiation from the particle surface.

Thus, the effect of the shape of particles on the velocity of their photophoretic motion has been studied only for some particular cases, while the temperature dependences of the transfer coefficients have been taken into account only under the approach implying the use of the exponential approximations. As has been shown in [12], this approximation may be used for describing the temperature dependences of the thermal conductivity and viscosity of a gas. However, for solid bodies, it appears, as a rule, to be either too rough or inapplicable at all. Therefore, it is of interest to develop a method for calculating the photophoresis velocity that would enable us to consider particles of complex shapes and avoid limitations on the pattern of the temperature dependences of viscosity and thermal conductivity.

The finite-element method is one of the methods free of tight limitations on the particle shape and the pattern of the temperature dependences of transfer coefficients. In this work, the finite-element method has been used to calculate the photophoresis velocities of solid aerosol particles, the sizes of which are much larger than the mean free path of gas molecules, under the conditions of the Reynolds and Peclet numbers equal to zero.

FORMULATION OF THE PROBLEM AND DESCRIPTION OF THE METHOD

According to the considered problem formulation, the distribution of temperature T_p inside an aerosol particle and the distributions of temperature T_g, velocities $\mathbf{u}$, and pressure p in a near-particle gas are described by the following equations [15–17]:

$$\nabla \cdot (\kappa_g \nabla T_g) = 0, \quad (1)$$

$$\nabla \cdot (\kappa_p \nabla T_p) = -f, \quad (2)$$

$$\nabla \cdot (\rho \mathbf{u}) = 0, \quad (3)$$

$$\nabla \cdot \boldsymbol{\sigma}(\mathbf{u}, p) = 0, \quad (4)$$

where the points denote the scalar products of vectors; κ_p and κ_g are the thermal conductivity coefficients of the particle material and gas, respectively; f is the power density of heat sources inside a particle; ρ is the gas density; and $\boldsymbol{\sigma}$ is the viscous stress tensor of the gas, which may, in the case under consideration, be expressed as follows:

$$\boldsymbol{\sigma}(\mathbf{u}, p) = 2\mu \mathbf{E}(\mathbf{u}) - p\mathbf{I} - \frac{2}{3}\mu \mathbf{I}(\nabla \cdot \mathbf{u}),$$

$$\mathbf{E}(\mathbf{u}) = \frac{1}{2}\left(\nabla \otimes \mathbf{u} + (\nabla \otimes \mathbf{u})^T\right).$$

Here, μ is the dynamic viscosity coefficient of the gas, $\mathbf{I}$ is the unit tensor, and symbol $\otimes$ denotes the tensor product of the vectors. In this work, an agreement is used, according to which the sign of the scalar multiplication may, sometimes, be omitted only upon the scalar multiplication of vectors and the multiplication of a scalar by a vector. The tensor and double scalar products are always denoted explicitly.

The gas density is assumed to be inversely proportional to the absolute temperature, while its dependence on pressure is ignored. The latter circumstance is due to the fact that, in the considered problem, the gas moves at velocities much lower than the velocity of sound, and variations in its pressure are small to compare with its average value. The following boundary conditions are imposed on the particle surface [17–19]:

$$T_g = T_p, \quad (5)$$

$$\kappa_p \mathbf{n} \cdot \nabla T_p - \kappa_g \mathbf{n} \cdot \nabla T_g = -\sigma_1 \sigma_0 \left(T^4 - T_\infty^4\right) + \varphi, \quad (6)$$

$$\mathbf{u} \cdot \mathbf{n} = 0, \quad (7)$$

$$\mathbf{u} \cdot \boldsymbol{\tau} = \frac{K_{TS}\mu}{T_g \rho} \boldsymbol{\tau} \cdot \nabla T_g. \quad (8)$$

Here, $\mathbf{n}$ is the normal directed from the surface of an aerosol particle inward it, i.e., out of the gaseous medium; $\boldsymbol{\tau}$ is an arbitrary unit tangential vector drawn from a considered point of the surface; K_{TS} is the thermal slip coefficient of the gas; T_∞ is the gas temperature at an infinite distance from the particle, this temperature being a constant preset value; σ_0 is the Stefan–Boltzmann constant; σ_1 is the integral degree of blackness; and φ is the surface density of internal heat sources. The penultimate term in Eq. (6) takes into account the heat radiation from the particle surface, and, in this form, it is applicable only in the absence of the energy transfer with the heat radiation from one regions of the surface to others, which imposes corresponding limitations on the possible shape of particles.

Let us consider in greater detail the φ value, which enters into Eq. (6). The radiation of widely used industrial lasers is absorbed by metals in a layer nearly

10^{-7} m thick [20]. For large aerosol particles, the layer thickness appears to be much smaller than their characteristic sizes. In this case, as will be shown below, the particle heating is more convenient to describe by the finite-element method, with the radiation absorption being taken into account in boundary condition (6) rather than using the bulk density of heat sources in Eq. (2). In this situation, the use of this term is a peculiarity of this work. This peculiarity has not previously been considered in the literature. This method of allowance for the surface heat sources may appear to be useful for solving the problems of evaporation, condensation, or combustion of aerosol particles.

The value of φ for a given particle material depends on the angle of incidence of the radiation onto the particle surface and the radiation wavelength. This value is calculated by the following equation:

$$\varphi = A|\mathbf{w} \cdot \mathbf{n}|,$$

where $\mathbf{w}$ is the flux-density vector of electromagnetic radiation incident onto the particle surface and A is the absorption ability of the particle material. The A values of some metals with respect to the electromagnetic radiation of different lasers can be found in [21].

A number of computer programs are, at present, available for numerical solution of an initial set of differential equations by the finite-element method with the use of a weak form of the formulation of such set. Freeware package with open software key freefem++ [22], which will be used in this work, is among such programs. In order to determine the temperature distribution and the gas velocity field in the vicinity of an aerosol particle using this approach, it is sufficient to find the corresponding weak forms of the formulation of the problems described by Eqs. (1)–(8). It is natural that the obtained expressions are desirable to be represented in a form convenient to use in the employed program. The program entails that an expression describing the problem formulation in a weak form may comprise only first-order derivatives of desired functions of coordinates. This limitation is relevant to the fact that the solution is sought as an expansion into a series in terms of basic functions that belong to the Sobolev first-order space.

Let us initially consider the procedure for calculating the temperature distribution inside and in the environment of an aerosol particle. According to the finite-element method, the distribution of any value is always sought in some finite region. Therewith, the entire region under examination is divided into a set of subregions. As a result, a computational grid is obtained, which is used to generate a set of basic functions. The computational grid must be selected in a manner such that the particle surface coincides with the boundaries of some subregions, which taken together form internal boundary Γ_S. Assume that the studied region is a sphere, with the particle located in its center. Therewith, constant temperature T_∞ is preset at external spherical boundary Γ_D of this region. In this way, a constant temperature is simulated at a large distance from the particle. It is obvious that the sizes of the calculation region must be rather large as compared with the particle size for the resulting velocity to be approximately equal to that reached in an infinite medium.

Now, we shall derive the weak form for the problem of temperature distribution. For this purpose, Eqs. (1) and (2) are written as the following unified equation:

$$\nabla \cdot (\kappa \nabla T) = -f, \tag{9}$$

where κ is the thermal conductivity; T is the substance temperature at the considered point, which may be located in both the gas and the particle; and f is the power density of the heat sources, which is nonzero only inside the particle.

Following the traditional approach [23], let us multiply the right- and left-hand sides of Eq. (9) by some test function ϕ, which is smooth in each subregion Ω_i; use the Green equation for each subregion; and, assuming that desired distribution of T is also described inside each subregion by a smooth function, we obtain the following [24]:

$$\int_\Omega f\phi dV = \int_\Omega \kappa(\nabla T)(\nabla \phi) dV + \sum_i \int_{\partial\Omega_i} (-\kappa \nabla T \mathbf{n}_i)\big|_{\Omega_i} \phi dS, \tag{10}$$

where $\partial\Omega_i$ is the boundary of subregion Ω_i; V is the volume; S is the area; and $\mathbf{n}_i$ is a vector external with respect to subregion Ω_i, with this vector being normal to the subregion boundary. Note that, upon the summation, each boundary between the subregions is taken into account two times. As has been mentioned above, the distributions of the desired values are commonly sought as expansions into series in terms of basic functions with unknown coefficients.

The test functions are used to obtain a set of equations for the calculation of the unknown coefficients. This set of equations is derived by consecutively substituting the test functions into the resulting expressions. If the test functions have been selected from the basic ones, while the basic functions are orthogonal, we deal with the Galerkin method [25].

In accordance with the conventional approach [25], a desired value distribution, which is preset for some parts of the calculation region boundary, is directly taken into account when constructing the set of equations, while the values of the test function in these parts are taken equal to zero. Therefore, at the external boundary with preset temperature T_∞, the ϕ value is equal to zero. As a result, all terms of the sum that are relevant to external boundary Γ_D are omitted in the last term of the right-hand side of Eq. (10). All

other terms of this sum may be divided into pairs in a manner such that the integrals of each pair may be united into one integral, the integrand of which will be the product of the test function and a change in the density of the heat flux through the interface between the subregions. At all internal boundaries, with the exception of the particle surface, this change is equal to zero. Therefore, the corresponding terms also vanish. At boundary Γ_S, the aforementioned change is specified by condition (6). Therewith, the use of the Sobolev function space for the approximation of the desired solution automatically ensures the continuity of the temperature distribution and, hence, the fulfillment of condition (5). As a result, we obtain the following weak form for determining the temperature distribution inside and in the vicinity of a particle:

$$\int_{\Omega} \tilde{f}\phi d\tilde{V} = \int_{\Omega} \tilde{\kappa}\left(\tilde{\nabla}\tilde{T}\right)\left(\tilde{\nabla}\phi\right)d\tilde{V} + \int_{(\partial\Omega_i \cap \Gamma_S)} \left(\frac{lT_\infty^3\sigma_1\sigma_0}{\kappa_{g\infty}}\left(\tilde{T}^4 - 1\right) - \frac{l\varphi}{\kappa_{g\infty}T_\infty}\right)\phi d\tilde{S}. \quad (11)$$

When writing this expression, we have passed to the following dimensionless variables:

$$\tilde{\kappa} = \frac{\kappa}{\kappa_{g\infty}}, \quad \tilde{T} = \frac{T}{T_{0\infty}}, \quad \tilde{f} = \frac{f}{T_\infty\kappa_{g\infty}}l^2.$$

Here, $\kappa_{g\infty}$ is the gas thermal conductivity at temperature T_∞ and l is the characteristic particle size. The tilde symbol over the operators, volume, and area indicates that the coordinates have been normalized with respect to characteristic size l.

Let us now derive the weak form used for determining the distribution of gas flow velocity in the vicinity of an aerosol particle and calculating its photophoresis velocity. When writing the corresponding expressions, the following dimensionless variables will be used:

$$\tilde{\mu} = \frac{\mu}{\mu_\infty}, \quad \tilde{p} = \frac{l}{U_0\mu_\infty}p, \quad \tilde{\mathbf{u}} = \frac{\mathbf{u}}{U_0}, \quad \tilde{\rho} = \frac{\rho}{\rho_\infty} = \frac{1}{\tilde{T}}, \quad (12)$$

where μ_∞ is the dynamic viscosity and ρ_∞ is the density of the gas at temperature T_∞, while $U_0 = \frac{K_{TS}\mu_\infty}{\rho_\infty l}$.

Using these variables, boundary conditions (7) and (8) may be represented in the form of the following unified expression:

$$\tilde{\mathbf{u}} = \tilde{\mu}\left(\tilde{\nabla}\tilde{T} - \left(\tilde{\nabla}\tilde{T}\cdot\mathbf{n}\right)\mathbf{n}\right). \quad (13)$$

It may be derived by applying the tangential projection operator [26] to expressions (7) and (8). This equation is more convenient than expressions (7) and (8) in the fact that the used software automatically calculates the components of vector **n**. After having determined the temperature distribution, the subregions corresponding to the internal parts of the particle may be excluded, and the velocity distribution may be calculated on the basis of a newly-constructed computational grid.

At the external boundary of the calculation region, the force applied to the gas from the side of the boundary is taken to be zero. Since the gas flow is assumed to be steady, its momentum remains unchanged with time. However, since conditions that do not affect the gas momentum have been imposed on the boundaries that do not concern the particle surface, the particle also does not change its momentum. Hence, the total particle–gas interaction force is equal to zero. Therefore, under these boundary conditions, we obtain a gas flow that results from the steady movement of the particle, with this flow being described in the reference system related to the particle. Since the sizes of the considered region are much larger than the particle size, we may conclude that the absolute value of the gas velocity at the boundary of the calculation region is equal to the absolute value of the particle velocity relative to the quiescent gas far from the particle.

From the formal point of view, expressions (3) and (4) are the Navier –Stokes equations for a compressible liquid [15, 16]. Note that, in the general case of using the finite-element method for a compressible liquid, another, so-called conservative, form of these equations is preferable. It yields a weak form, which does not comprise the density in the explicit form, with the kinematic viscosity and the momentum flux density of a liquid or a gas rather than the dynamic viscosity and velocity being used for this purpose [27]. Expressions (3) and (4) yield the weak form, the use of which for a compressible liquid may, in the general case, lead to multiple or incorrect solutions [27]. However, since the density–pressure dependence is not, in our case, taken into account, the same method may be employed to obtain the weak form as that used for an incompressible liquid on the basis of the written equations, while the density may be excluded with the help of relation (12). In this work, the above approach will be employed, because it is simpler than the general method based on the conservative form.

Multiplying Eqs. (3) and (4) by scalar q and vector **v** test functions and using the standard transformations [25] with allowance for Eqs. (12) and (13), we arrive at

$$\int_{\Omega}\left[2\tilde{\mu}\tilde{\mathbf{E}}(\tilde{\mathbf{u}}) : \tilde{\mathbf{E}}(\tilde{\mathbf{u}}) - \left(\tilde{p} + \frac{2}{3}\tilde{\mu}\left(\tilde{\nabla}\cdot\tilde{\mathbf{u}}\right)\right)\tilde{\nabla}\cdot\mathbf{v}\right]d\tilde{V} + \int_{\Omega} q\tilde{\nabla}\cdot\left(\frac{1}{\tilde{T}}\tilde{\mathbf{u}}\right)d\tilde{V} = 0. \quad (14)$$

CALCULATION OF PHOTOPHORESIS VELOCITY FOR AXIALLY SYMMETRIC PARTICLES

Let us formulate the above-described general calculation scheme more specifically for the photophoresis velocity of axially symmetric particles. As has been mentioned above, according to the finite-element method, the distribution of any value is searched for in the form of the expansion into a series in terms of basic functions, while entire studied region Ω is divided into a set of subregions. Therewith, each basic function is nonzero only in some neighboring subregions. Therefore, the more accurately the desired distribution is to be extrapolated the larger number of subregions is required. Hence, rather large computational resources are needed to find such distributions. If the desired distributions are axially symmetric, which is the case, the requirements for computational resources may be decreased many times by passing to cylindrical coordinates and reducing the three-dimensional problem to the two-dimensional one, in which all distributions depend only on polar radius r and applicate z of a cylindrical coordinate system. The relations necessary for the passage to the cylindrical coordinate system in Eqs. (11) and (14) have been presented in [25], while the examples of the calculations with the use of this approach are reported in [22]. In view of the simplicity of these transformations, they are not described here.

Let us now consider the construction of the computational grid and the procedure of calculations based on the latter. To be more specific, we shall consider that the particle has the shape of a spheroid. The structure of the calculation region is shown in Fig. 1. To make the representation of individual elements more convenient, the ratios between their sizes differ from the really used ones. Let symbol a denote the distance from the center of the particle to its surface along the z axis, while symbol b reflects the distance from the particle center to its surface in the direction perpendicular to this axis. When constructing the computational grid, distance b was taken as unity, while the real value of this distance was used as characteristic size l in Eqs. (11) and (14). At $a \le b$, the distance from the particle center to the boundary of the calculation region was assumed to be $1000b$; in the opposite case, it was $1000a$. The region under consideration was divided into subregions using the Delone–Voronoi algorithm [28]. The freefem++ software performs this dividing automatically in accordance with a preset number of points at the boundaries. The number of the points was selected to be sufficient for reaching desirable calculation accuracy. Therewith, it was assumed that relative error ε_Δ in calculating the absolute value of photophoresis velocity U of the particle satisfied the following conditions:

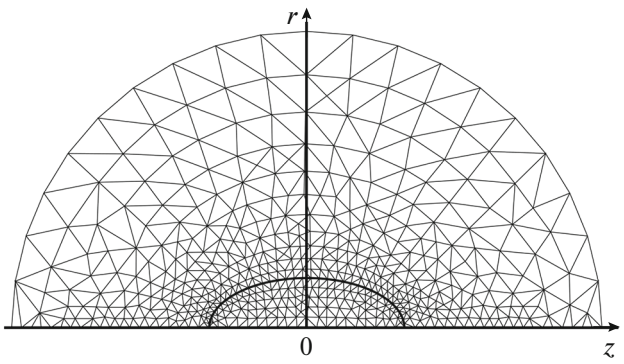

Fig. 1. Structure of calculation region.

$$\varepsilon_\Delta < \left| \frac{\int\limits_{\Gamma_S} \left| \tilde{\mathbf{u}} \cdot \boldsymbol{\tau} - \tilde{\mu} \tilde{\nabla} \tilde{T} \cdot \boldsymbol{\tau} \right| dS}{\int\limits_{\Gamma_S} \tilde{\mu} \tilde{\nabla} \tilde{T} \cdot \boldsymbol{\tau} dS} \right|, \quad \varepsilon_\Delta < \frac{\int\limits_{\Gamma_D} |U - u| dS}{U}.$$

The validity of these inequalities was confirmed by test calculations (see below). In the calculations, the sought absolute value of the photophoresis velocity of the particle was taken equal to the average absolute value of the gas velocity at the external boundary of the calculation region. In order to control the accuracy, the gas velocities were also calculated at the points of intersection between this boundary and the r and z axes. All these velocities must coincide with each other within the selected accuracy, provided that the calculation is performed correctly. Moreover, the control over the accuracy was implemented by performing the calculations using different variants of dividing the calculation region into the subregions, including different numbers of the latter. The desired temperature distribution was approximated using basic functions derived from the second-order Legendre polynomials.

Note that the temperature distribution may be directly obtained using weak form (11), provided that normalized thermal conductivity $\tilde{\kappa}$ is dependent only on the coordinates and independent of the temperature. The calculation with regard to the dependence of the thermal conductivity on temperature is performed using the iteration refinement of its distribution on the basis of the Newton or Picard method [29]. The Picard method was used in this work. According to this method, the temperature distribution was initially found at thermal conductivity $\tilde{\kappa}$ calculated for each point at temperature T_∞. Then, the calculation of the temperature distribution was repeated at given $\tilde{\kappa}$ calculated for each point from the temperature at this point found at the previous step. After that, the procedure was repeated until a change in normalized temperatures $\tilde{T}$ at different control points of the calculation region became smaller than some preset value. In this work, this value was taken equal to 10^{-4}. Having

determined the temperature distribution, the subregions corresponding to the internal regions of the particle were excluded, and the velocity distribution was calculated on the basis of the newly-constructed calculation grid.

When considering radiation absorption by an infinitely thin surface layer of the particle, it was assumed that the radiation flux is directed along the z axis. Velocity and pressure fields were approximated using the third- and second-order Legendre polynomials, respectively. The calculation procedure for the velocity and pressure fields coincided with that used in [30] and is not described here.

CALCULATION RESULTS

Let us initially consider the results of test calculations that confirm the validity of the developed procedure. An analytical equation describing the dependence for the photophoresis velocity of a spherical particle at low temperature drops was derived in [5]. To test the proposed method, the photophoresis velocities were calculated by the formulas derived in that work at different transfer coefficients for the case of the complete absorption of an incident radiation by an infinitely thin surface layer of a particle and for a model situation, in which the volume density of internal heat sources is proportional to the value of the z coordinate. The calculations were performed at radiation intensity or volume densities of internal sources that increased the mean temperature of the particle surface by only a few fractions of a degree. In both cases, the calculation results obtained by the equations obtained in [5] and on the basis of the method considered in this work have appeared to differ by no more than 0.1%. An equation derived in [7] was used to perform analogous calculations for a flattened spheroid under the condition of the absorption of an incident radiation by an infinitely thin surface layer of a particle. The results of the calculations carried out on the basis of this equation for the case, in which the major semiaxis is longer than the minor one by no more than ten times, have appeared to differ from those obtained by the method considered in this work by no more than 0.7%.

The authors of [8] have reported the results of calculating the photophoresis velocity of a copper particle 25 μm in radius for high temperature drops with allowance for the heat radiation from its surface. The temperature dependences of the molecular-transfer coefficients were described by power functions, and it was assumed that $\sigma_1 = 1$. The data presented graphically in [8] have coincided (within their accuracy) with the results of testing calculations performed in terms of the method proposed in this work.

To illustrate the potential of the calculation scheme, the photophoresis velocities were calculated for particles of three shapes: a cylinder, a spheroid, and a shape resulting from rhomb rotation around its diagonal (Fig. 2). We shall refer to this configuration as a doubled cone. In all cases, it was assumed that the radiation incident onto the particles was absorbed by their thin surface layers. The particles were considered to move in air at temperature $T_\infty = 300$ K, a pressure at a large distance from the particles of 10^5 Pa, $\rho_\infty = 1.177$ kg/m^3, and $K_{TS} = 1.152$ [19]. For air thermal conductivity, the following temperature dependence was used (here and below, the temperature was measured in absolute degrees):

$$\kappa_g = (2.819\times10^{-11}T^3 - 7.832\times10^{-8}T^2 + 1.219\times10^{-4}T - 4.244\times10^{-3})\frac{\text{W}}{\text{mK}},$$

which was obtained from the data of [31] and, within a range of 300–1100 K, agreed with these data with an accuracy of 0.6%. For air viscosity, the following approximation [32] was employed:

$$\mu = \left(1.7162\times10^{-5}\frac{384}{111+T}\left(\frac{T}{273}\right)^{1.5}\right)\text{ Pa s},$$

which described the data presented in [33] for temperature ranges of 270–900 and 900–1200 K with accuracies of 0.4 and 2%, respectively. Copper and vanadium particles were considered. For copper thermal conductivity, the following approximation was used:

$$\kappa_p = (-0.0681T + 420.47)\frac{\text{W}}{\text{mK}},$$

which was obtained from the data of [34], and, in a temperature range of 300–1200 K, agreed with these data at an accuracy of 0.3%. For vanadium thermal conductivity, the following dependence was employed:

$$\kappa_p = (5.91\times10^{-12}T^4 - 3.12\times10^{-8}T^3 + 5.60\times10^{-5}T^2 + 2.59\times10^{-2}T - 34.1)\frac{\text{W}}{\text{mK}},$$

which was obtained from the data of [34], and, in a temperature range of 300–2000 K, agreed with these data at an accuracy of 0.7%. Particles with $b = 25$ and 10 μm were studied in this work. As has been mentioned above, the effect of the heat radiation increases with the particle size. To estimate this effect, the velocities of spheroidal copper particles with $\sigma_1 = 1$ and $\sigma_1 = 0$ were calculated. The calculations have shown that, at a preset Aw value, the effect of the heat radiation increases with a decrease in the a/b ratio, and, for a particle with $a/b = 0.1$ heated by radiation to 1200 K, allowance for the heat radiation leads to a decrease in the particle velocity and surface temperature by 1.4 and 2.3%, respectively. Thus, for particles with the sizes under consideration, the effect of the

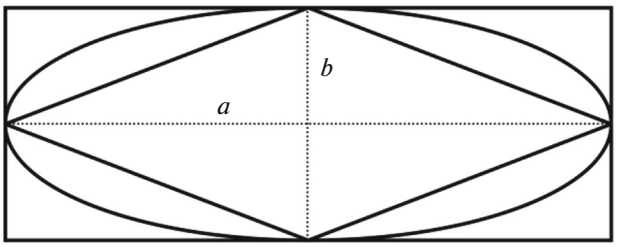

Fig. 2. Cross-sectional shapes of particles under consideration.

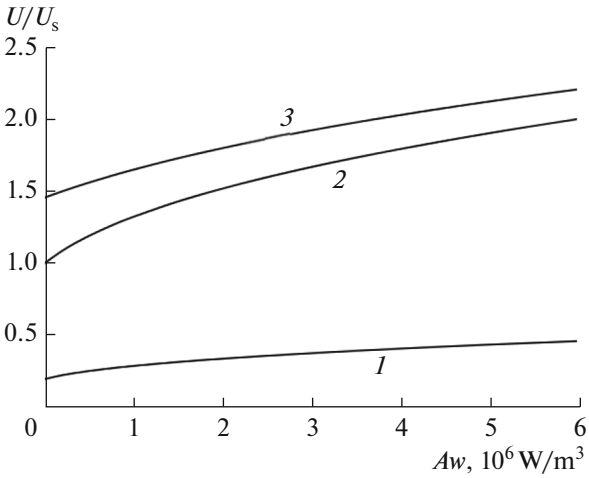

Fig. 3. Dependences of photophoresis velocity on radiation power for spheroidal copper particles at different semiaxial ratios: a/b = (*1*) 0.1, (*2*) 1, and (*3*) 10.

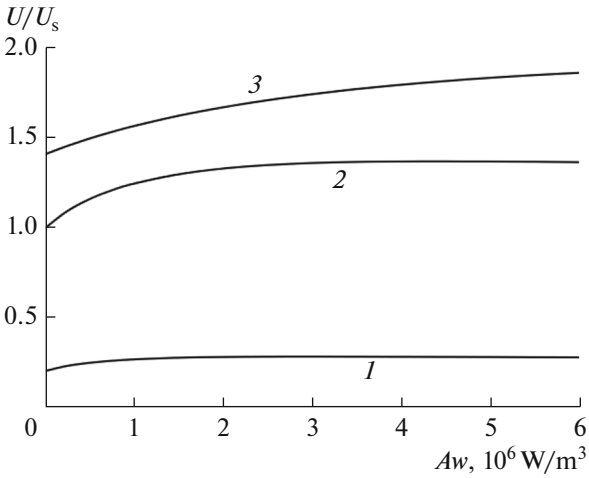

Fig. 4. The same as in Fig. 3 for vanadium particles.

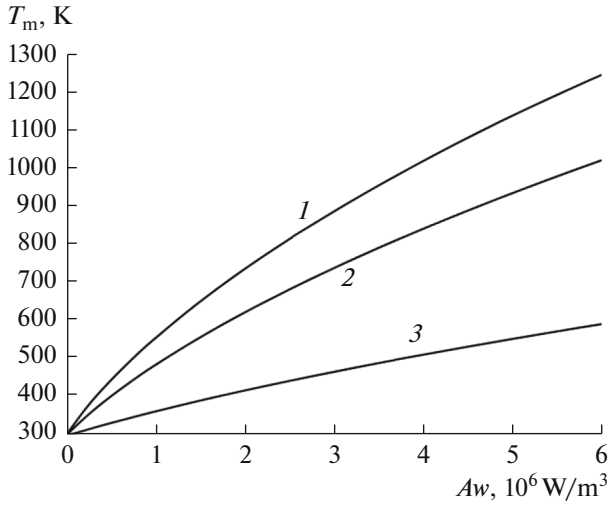

Fig. 5. Dependences of mean temperature on radiation power for spheroidal particle (b = 25 μm) at different semiaxial ratios: a/b = (*1*) 0.1, (*2*) 1, and (*3*) 10.

heat radiation is rather weak, and a specific σ_l value does not have an essential influence on the analysis of the behavior of a particle. For metals, σ_l value is, generally speaking, dependent on the temperature of a body surface, its smoothness, and degree of oxidation. Depending on conditions, it may vary from actually zero to nearly unity. To be more specific, in all subsequent calculations it was taken to be $\sigma_l = 1$.

The dependences of the particle velocity on the incident radiation intensity and changes in the thermal conductivity of particle material with temperature are illustrated in Figs. 3 and 4. Figures 3 and 4 present the data on copper and vanadium particles, respectively. It should be noted that, as the temperature is elevated, the thermal conductivity of copper and vanadium decreases and increases, respectively. The particle velocities were normalized with respect to the U_s value found for a spherical particle with no regard to its heating and heat radiation from its surface [5]:

$$U_s = \frac{K_{TS}\mu_\infty}{T_\infty \rho_\infty} \frac{Aw}{3(2\kappa_g - \kappa_p)}.$$

For copper and vanadium particles 25 μm in radius, the values of this velocity normalized with respect to Aw are $5.02\times10^{-11}\,\mathrm{m}^3/(\mathrm{W\ s})$ and $6.56\times10^{-10}\,\mathrm{m}^3/(\mathrm{W\ s})$, respectively.

Figure 5 shows the dependences of mean temperature T_m of a particle surface on Aw. This figure presents the data on copper particles; however, they are similar for vanadium particles. In order to show the effects of particle shape and size on the photophoresis velocity, Table 1 presents the data calculated for copper particles at $Aw = 5\times10^6\,\mathrm{W/m}^2$. The velocity val-

Table 1. Photophoresis velocity (μm/s) of copper particles with different shapes at $Aw = 5\times10^6$ W/m^2; parenthetic numerals denote the mean temperatures of particle surface (in absolute degrees)

a/b	Cylinder	Spheroid	Doubled cone
$b = 10$ μm			
0.1	150 (718)	88.9 (743)	–
0.5	276 (637)	287 (680)	263 (723)
1	316 (585)	385 (627)	273 (681)
5	389 (454)	471 (477)	504 (508)
10	398 (407)	456 (421)	464 (440)
$b = 25$ μm			
0.1	191 (1100)	113 (1144)	–
0.5	345 (956)	362 (1034)	327 (1111)
1	391 (862)	482 (940)	344 (1036)
5	465 (619)	567 (662)	614 (722)
10	465 (529)	537 (556)	551 (594)

Table 2. Normalized photophoresis velocity of copper particles with different shapes at $Aw = 10^4$ W/m^2, $b = 25$μm

a/b	Normalized velocity		
	cylinder	spheroid	doubled cone
0.5	0.711	0.715	0.633
1	0.850	1.01	0.675
5	1.20	1.42	1.47
10	1.30	1.47	1.46

ues that could not be calculated with the required accuracy are omitted in the table. As can be seen from the table, at low a/b values, an increase in this ratio leads to the growth of the velocity; however, at high a/b values, the velocity may decrease as well. Note that the main role in the decrease within the considered range of a/b values and at the given radiation intensity is played by a reduction in the mean particle temperature. To illustrate this fact, Table 2 lists the normalized photophoresis velocities of copper particles at $Aw = 10^4$ W/m^2. In this case, the maximum deviation of the mean temperature from the ambient temperature is no higher than 4 K. The particle velocities were normalized relative to spherical particle velocity calculated with no allowance for its heating and the heat radiation from its surface.

ACKNOWLEDGMENTS

This work was supported the Ministry of Education and Science of the Russian Federation (research no. 576) within the framework of the basic part of a State Assignment in the field of scientific work, no. 2014/700, 2014.

REFERENCES

1. Ehrenhaft, F., *Ann. Phys.* (New York), 1918, vol. 55, p. 81.
2. Kutukov, V.B., Shchukin, E.R., and Yalamov, Yu.I., *Zh. Tekh. Fiz.*, 1976, vol. 46, p. 626.
3. Reed, L.D., *J. Aerosol Sci.*, 1977, vol. 8, p. 123.
4. Arnold, S. and Lewittes, M., *J. Appl. Phys.*, 1982, vol. 53, p. 5314.
5. Yalamov, Yu.I. and Khasanov, A.S., *Zh. Tekh. Fiz.*, 1998, vol. 68, no. 4, p. 1.
6. Keh, H.J. and Tu, H.J., *Colloids Surf. A*, 2001, vol. 176, no. 2, p. 213.
7. Malai, N.V., Mironova, N.N., and Shchukin, E.P., *J. Eng. Phys. Thermophys.*, 2008, vol. 81, p. 989.
8. Malai, N.V., Limanskaya, A.V., Shchukin, E.R., and Stukalov, A.A., *Zh. Tekh. Fiz.*, 2012, vol. 82, no. 10, p. 42.
9. Horvath, H., *KONA Powder Part. J.*, 2014, vol. 31, p. 181.
10. Ou, C.L. and Keh, H.J., *J. Colloid Interface Sci.*, 2005, vol. 282, p. 69.
11. Malay, N.V., Mironova, N.N., and Shchukin, E.R., *Univ. J. Phys. Appl.*, 2014, vol. 8, p. 251.
12. Pleskanev, A.A., *Cand. Sci. (Phys.-Math.) Dissertation*, Belgorod: Belgorod State Univ., 2006.
13. Malai, N.V., Limanskaya, A.V., Shchukin, E.R., and Stukalov, A.A., *Opt. Atmos. Okeana*, 2012, vol. 25, p. 335.
14. Loesche, C. and Husmann, T., *J. Aerosol Sci.*, 2016, vol. 102, p. 55.
15. Happel, J. and Brenner, H., *Low Reynolds Number Hydrodynamics*, Leiden: Noordhoff, 1965.
16. Landau, L.D. and Lifshitz, E.M., *Fluid Mechnics*, Oxford: Pergamon Press, 1987.
17. Samarskii, A.A. and Vabishchevich, P.N., *Vychislitel'naya teploperedacha* (Computing Heat Transfer), Moscow: Editorial URSS, 2003.
18. Brock, J.R., *J. Colloid Sci.*, 1962, vol. 17, p. 768.
19. Poddoskin, A.B., Yushkanov, A.A., and Yalamov, Yu.I., *Zh. Tekh. Fiz.*, 1982, vol. 52, p. 2253.
20. Veiko, V.P., Libenson, M.N., Chervyakov, G.G., and Yakovlev, E.B., *Vzaimodeistvie lazernogo izlucheniya s veshchestvom. Silovaya optika* (Laser Radiation Interaction with Matter. Power Optics), Moscow: FIZMATLIT, 2008.
21. Klimkov, Yu.M., Maiorov, V.S., and Khoroshev, M.V., *Vzaimodeistvie lazernogo izlucheniya s veshchestvom: uchebnoe posobie* (Laser Radiation Interaction with Matter: A Manuel), Moscow: MIIGAiK, 2014.
22. Hecht, F., *J. Numer. Math.*, 2012, vol. 20, p. 251.
23. Girault, V. and Wheeler, M.F., in *Partial Differential Equations. Modeling and Numerical Simulation*, Glowinski, R. and Neittaanmäki, P., Eds., Berlin: Springer, 2008, p. 3.

24. Carnes, B.R. and Copps, K.D., *Thermal Contact Algorithms in SIERRA Mechanics*, Albuquerque: Sandia National Laboratories, 2008.

25. Reddy, J.N. and Gartling, D.K., *The Finite-Element method in Heat Transfer and Fluid Dynamics*, Boca Raton: CRC, 2010.

26. Glowinski, R., *Numerical Methods for Fluids. Part 3*, Amsterdam: Elsevier, 2003, vol. 9.

27. Zienkiewicz, O.C., Taylor, R.L., and Nithiarasu, P., *The Finite-Element Method for Fluid Dynamics*, Oxford: Butterworth-Heinemann, 2014, p. 7.

28. Lucquin, B. and Pironneau, O., *Introduction to Scientific Computing*, Chichester: Wiley, 1998.

29. Logg, A., Mardal, K.A., and Wells, G., *Automated Solution of Differential Equations by the Finite-Element Method*, Berlin: Springer Science & Business Media, 2012.

30. Grashchenkov, S.I., *Colloid J.*, 2017, vol. 79, p. 35.

31. Vargaftik, N.B., Filippov, L.P., Tarzimanov, A.A., and Totskii, E.E., *Spravochnik po teploprovodnosti zhidkostei i gazov* (Handbook on Thermal Conductivity of Liquid and Gases), Moscow: Energoatomizdat, 1990.

32. Rabinovich, G.G., Ryabykh, P.M., Khokhryakov, P.A., Molokanov, Yu.K., and Sudakov, B.N., *Raschety osnovnykh protsessov i apparatov neftepererabotki* (Computing of the Basic Processes and Apparata of Oil Refining), Moscow: Khimiya, 1979.

33. Vargaftik, N.B., *Spravochnik po teplofizicheskim svoistvam gazov i zhidkostei* (Handbook on Thermophysical Properties of Gases and Liquids), Moscow: Nauka, 1972.

34. Zinov'ev, V.E., *Teplofizicheskie svoistva metallov pri vysokikh temperaturakh. Spravochnik* (Thermophysical Properties of Metals at High Temperatures), Moscow: Metallurgiya, 1989.

Translated by A. Kirilin